universe

MDPI

Article

Unconventional Mechanisms of Heavy Quark Fragmentation

Boris Kopeliovich [1,*], Jan Nemchik [2,3], Irina Potashnikova [1] and Ivan Schmidt [1]

[1] Departamento de Física, Universidad Técnica Federico Santa María, Avenida España 1680, Valparaíso 2390123, Chile; irina.potashnikova@usm.cl (I.P.); ivan.schmidt@usm.cl (I.S.)
[2] Faculty of Nuclear Sciences and Physical Engineering, Czech Technical University in Prague, Břehová 7, 11519 Prague, Czech Republic; jan.nemcik@fjfi.cvut.cz
[3] Institute of Experimental Physics SAS, Watsonova 47, 04001 Košice, Slovakia
* Correspondence: boris.kopeliovich@usm.cl

Abstract: Heavy and light quarks produced in high-p_T partonic collisions radiate differently. Heavy quarks regenerate their color field, stripped-off in the hard reaction, much faster than the light ones and radiate a significantly smaller fraction of the initial quark energy. This peculiar feature of heavy-quark jets leads to a specific shape of the fragmentation functions observed in e^+e^- annihilation. Differently from light flavors, the heavy quark fragmentation function strongly peaks at large fractional momentum z, i.e., the produced heavy–light mesons, B or D, carry the main fraction of the jet momentum. This is a clear evidence of the dead-cone effect, and of a short production time of a heavy–light mesons. Contrary to propagation of a small $q\bar{q}$ dipole, which survives in the medium due to color transparency, a heavy–light $Q\bar{q}$ dipole promptly expands to a large size. Such a big dipole has no chance to remain intact in a dense medium produced in relativistic heavy ion collisions. On the other hand, a breakup of such a dipole does not affect much the production rate of $Q\bar{q}$ mesons, differently from the case of light $q\bar{q}$ meson production.

Keywords: quarks; jets; fragmentation; hadronization

check for updates

Citation: Kopeliovich, B.; Nemchik, J.; Potashnikova, I.; Schmidt, I. Unconventional Mechanisms of Heavy Quark Fragmentation. *Universe* **2023**, *9*, 418. https://doi.org/10.3390/universe9090418

Academic Editors: Sevil Salur, Fridolin Weber and Christine Nattrass

Received: 28 July 2023
Revised: 20 August 2023
Accepted: 10 September 2023
Published: 13 September 2023

1. Introduction

Particles produced in hard hadronic collisions are detected at macroscopic distances from the collision area, so they carry only indirect information about the dynamics at the early stage of fragmentation. Nuclear targets provide a unique opportunity to probe the early stage of fragmentation at distances of a few Fermi from the origin. A quark–gluon system originating from the hard collision propagates through the nuclear medium and interacts with other nucleons. Nuclear modification of the differential cross section of particle production can bring forth precious information about the structure of the excited system and its space–time development.

The non-perturbative models of color charge fragmentation usually are based on the string models, which was first proposed in [1]. As a manifestation of the concept of confinement, the separated color charges are connected with color-flux tubes, which frequently are replaced by color strings, because the transverse size of the tubes is much less than their length [2]. Monte-Carlo events generators based on the models for string fragmentation (e.g., [3]) are frequently used to simulate the distributions of produced particles. These models however, provide no space–time pattern of jet development, but only the final hadron distribution. Exceptional is the study of time development performed in [4], which confirmed the unusual space–time behavior of leading hadron production, proposed earlier in [5].

The important feature of string fragmentation is the constant rate of energy dissipation in vacuum (not medium induced),

$$\frac{dE}{dL} = -\kappa, \quad (1)$$

where L is the path length; κ is the string tension, i.e., the string field energy per unit of length [1].

For hard reactions a perturbative treatment of fragmentation [2,6,7] looks more appropriate. In particular, a high-p_T parton scattering leads to formation of four cones of gluon radiation: (i)–(ii) backward–forward jets formed by the color field of the colliding partons shaken off in the hard collision; (iii)–(iv) the scattered partons carry no field up to transverse momenta $k_T < p_T$. These partons are regenerating the lost color field via gluon radiation forming the up-down jets, as is illustrated in Figure 1.

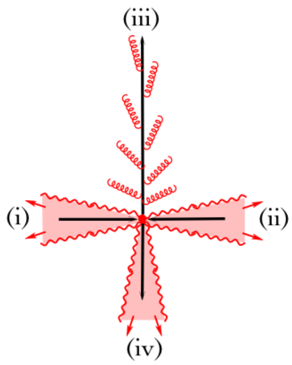

Figure 1. High-p_T collision in the c.m. frame of two partons, which leads to production of four jets: (i,ii) soft color field shaken off in the collision; (iii,iv) transverse cones of gluons radiated due to regeneration of the stripped off color field.

The radiational process is ordered in time or path length according to [8],

$$l_c = \frac{2Ex(1-x)}{k_T^2 + x^2 m_q^2} \,. \tag{2}$$

Here x is the fractional light-cone momentum of the radiated gluon; k_T is its transverse momentum relative to the initial quark direction. The radiated gluons subsequently hadronize forming a jet of hadrons. For heavy quarks the second term in the denominator plays important role leading to the so called dead-cone effect [9].

In terms of the Fock state representation all radiated gluons pre-exist in the initial bare parton, and are liberated on mass shell successively in accordance with their coherence length/time Equation (2). First are radiated gluons with small longitudinal and large transverse momenta.

Radiational Energy Loss in Vacuum

Amazing feature of energy loss for gluon radiation is analogy to the string model, its rate is constant, like in (1) [10]. How much energy is radiated over the path length L? Only gluons with radiation length $l_c < L$ contribute [11],

$$\Delta E_{rad}(L) = \int\limits_{\lambda^2}^{Q^2} dk_T^2 \int\limits_0^1 dx\, \omega\, \frac{dn_g}{dx\, dk_T^2}\, \Theta(L - l_c), \tag{3}$$

where ω is the gluon energy; the soft cut-off parameter $\lambda = 0.2\,\text{GeV}$. The perturbative radiation spectrum reads,

$$\frac{dn_g}{dx\, dk_T^2} = \frac{2\alpha_s(k_T^2)}{3\pi\, x}\, \frac{k_T^2[1+(1-x)^2]}{[k_T^2 + x^2 m_Q^2]^2} \,. \tag{4}$$

We see that radiation by light and heavy quarks behave quite differently at small k_T:

(i) Light quarks: $dn_g/dk_T^2 \propto 1/k_T^2$.
(ii) Heavy quarks: $dn_g/dk_T^2 \propto k_T^2/m_Q^2$.

Dead-cone effect: gluons with $k_T^2 < x^2 m_Q^2$ are suppressed [9,11]. Heavy quarks radiate less energy compared with the light ones. They promptly restore their color field and stop radiating. The amount of radiated energy for light and heavy flavors is depicted in Figure 2 vs. radiation length for different jet energies.

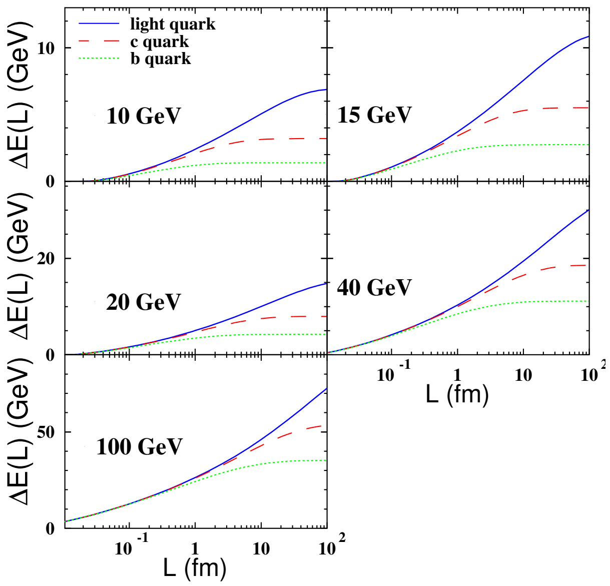

Figure 2. Radiational energy loss in vacuum by light (u, d), c and b quarks, depicted by blue, red and green curves respectively. Radiated energy ΔE is plotted as function of path length for different jet energies.

We see that heavy quarks radiate only a small fraction 10–20% of their initial momentum. In particular, this explains the unusual shape of the experimentally observed fragmentation function $D_{b/B}(z)$ of b-quarks, presented in Figure 3 [12] (and similar for charm [13]).

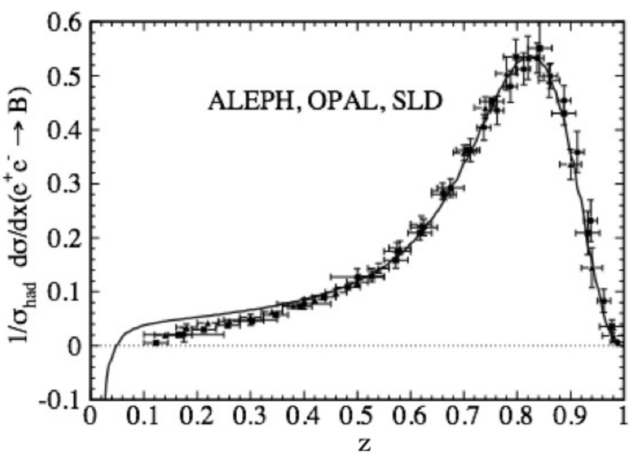

Figure 3. The $b \to B$ fragmentation function, from e^+e^- annihilation at LEP. The curve is the DGLAP fit [12].

Indeed, most of B-mesons carry a large fraction z∼80%, of the b-quark momentum.

We conclude that such a specific shape of the fragmentation function of heavy quarks is a direct manifestation of the dead-cone effect.

2. Production Length

The process of gluon radiation by a heavy quark Q ends up with color neutralization by a light antiquark and production of a $Q\bar{q}$ dipole. As far as we are able to calculate the radiated fraction of the light-cone momentum (e.g., for b-quark) $\Delta p_+^b(L)/p_+^b$, the production length L_p distribution $W(L_p)$ can be extracted directly from data on $D_{b/B}(z)$,

$$\frac{dW}{dL_p} = \left.\frac{\partial \Delta p_+^b(L)/p_+^b}{\partial L}\right|_{L=L_p} D_{b/B}(z)\,, \tag{5}$$

The results for the differential distribution dW/dL_p are depicted in Figure 4 at several values of momenta p_T.

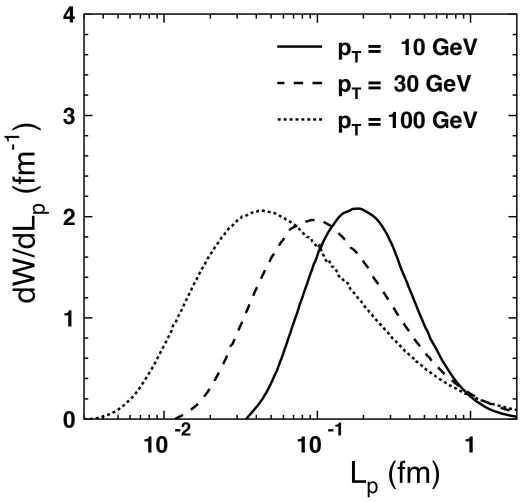

Figure 4. The L_p-distribution of B-mesons produced with different p_T in pp collisions.

Remarkably, the mean value of L_p is extremely short and shrinks with rising p_T. This sounds counter-intuitive, however, the process has maximal hard scale allowed by the kinematics $p_T = E_{c.m.}/2$.

The production length L_p turns out to be much shorter than the confinement radius, indicating that the fragmentation mechanism is pure perturbative. At $L = L_p$, a small-size dipole $b\bar{q}$ is produced, with no certain mass, but with a certain radius. It is to be projected on the B-meson wave function, giving $\Psi_B(0)$ (compare with [14]).

3. Fragmentation in a Dense Medium

3.1. Formation Length of a $Q\bar{q}$ Meson

The light antiquark in the B-meson carries a tiny fraction of its momentum, $x \approx m_q/m_Q$, i.e., about 5%. The produced $b\bar{q}$ dipole has a small transverse separation, but it expands with a high speed, enhanced by $1/x$, i.e., is an order of magnitude faster than symmetric $\bar{q}q$ or $\bar{Q}Q$ dipoles.

$$l_f \sim \frac{1}{2} x(1-x)\langle r_T^2\rangle p_T, \tag{6}$$

where $\langle r_T^2\rangle = 8/3\langle r_{ch}^2\rangle$, and $\langle r_{ch}^2\rangle_B = 0.378\,\text{fm}^2$ as was evaluated in the potential model [15]. The B meson is nearly as big as the pion, since its radius is controlled by the mass of the light antiquark.

According to (6) the dipole heavy–light $Q\bar{q}$ dipole separation promptly reaches the large hadronic size. This is confirmed by comparison data, for J/ψ detected in $Pb-Pb$ nuclear collisions. Data demonstrate color opacity for B-mesons (non-prompt J/ψ production) and color transparency for J/ψ (prompt production). The nuclear suppression factors R_{AA} for these two channels are compared in Figure 5 [16].

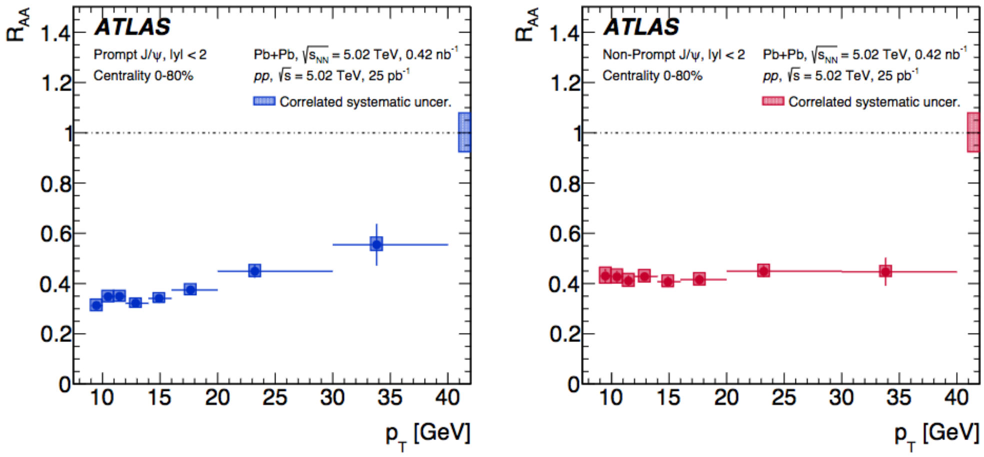

Figure 5. Nuclear suppression factor R_{AA} vs. p_T. (**Left**): promptly produced J/ψ's exhibit color transparency effect. (**Right**): J/ψ's from B decays demonstrate a p_T-independent color-opacity effect.

While Equation (6) describes the early, perturbative stage of the dipole expansion, the further evolution filters out the states with large relative phase shifts. The longest time takes discrimination between the two lightest hadrons, the ground state B and the first radial excitation B', which concludes the formation process. Correspondingly, the full formation path length can be evaluated as,

$$l_f = \frac{2p_T}{m_{B'}^2 - m_B^2}. \tag{7}$$

E.g., for the oscillatory potential $m_{B'} - m_B = 0.6\,\text{GeV}$, so $l_f = 0.06\,\text{fm}[p_T/1\,\text{GeV}]$ is extremely short for medium–large transverse momenta.

3.2. Attenuation of Dipoles Propagating in a Dense Medium

The mean free path of a $Q - \bar{q}$ meson in a hot medium characterizing by the transport coefficient (the rate of broadening) $\hat{q}$,

$$\lambda_{Q\bar{q}} \sim \frac{1}{\hat{q}\langle r_T^2\rangle} = \frac{3}{8\hat{q}\langle r_{ch}^2\rangle_{Q\bar{q}}}. \tag{8}$$

E.g., at $\hat{q} = 1\,\text{GeV}^2/\,\text{fm}$ $\lambda_B = 0.04\,\text{fm}$, so a formed B-meson breaks up in the medium nearly instantaneously.

A b-quark propagating through the hot medium, easily picks up and loses accompanying light antiquarks without an essential reduction of its momentum. Meanwhile the b-quark keeps dissipating its energy with a rate, slightly enhanced by medium induced radiative energy loss [17] effects. Eventually the detected B-meson is produced in the dilute periphery of the medium.

The heavy quark keeps losing energy even inside a colorless $Q\bar{q}$ dipole sharing its momentum with the light quark, as is illustrated in Figure 6 presenting a unitarity cut of a $\bar{q}q$ Reggeon.

Thus, the heavy quark Q dissipates a part of its energy on a long path from the hard collision point to the medium periphery.

$$\frac{dE}{dL} = \frac{dE_{rad}}{dL} - \kappa(T), \tag{9}$$

where $\kappa(T)$ is temperature dependent string tension in the medium [18] $\kappa(T) = \kappa_0(1 - T/T_c)^{1/3}$; the vacuum string tension $\kappa_0 = 1\,\text{GeV}/\,\text{fm}$; The critical temperature is fixed at $T_c = 200\,\text{MeV}$.

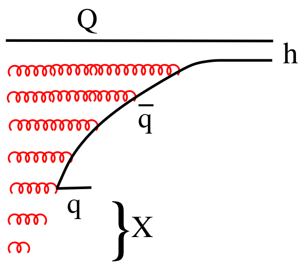

Figure 6. Redistribution of energy inside the $Q\bar{q}$ dipole. The gluons radiated by Q are absorbed by $\bar{q}$ so the dipole energy remains unchanged.

3.3. Medium Modified Production Rate

The cross section of a heavy–light meson M production in pp collisions can be presented in the factorized form,

$$\frac{d^2\sigma_{pp\to M}}{d^2p_T} = \frac{1}{2\pi p_T E_T}\int d^2q_T\,\frac{d^2\sigma_{pp\to Q}}{d^2q_T}\int\limits_0^\infty dL_p\frac{dW}{dL_p}\,\frac{\Delta E(L_p)}{E}\,\delta\left(1-z-\frac{\Delta E(L_p)}{E}\right) \quad (10)$$

We replaced the $b \to B$ fragmentation function by the differential expression (5). The medium-modified L_p distribution is given by,

$$\frac{dW^{AA}}{dL_p} = \frac{1}{2}\langle r_B^2\rangle\hat{q}(L_p)\,\exp\left[-\frac{1}{2}\langle r_B^2\rangle\int\limits_{L_p}^\infty dL\,\hat{q}(L)\right] \quad (11)$$

Here, for the sake of simplicity, we fixed the $Q\bar{q}$ dipole separation at the mean value. This approximation is rather accurate due to shortness of l_f. Otherwise, one can calculate the attenuation factor in (11) exactly, applying the path integral technique [19,20].

Eventually, the production rate of heavy–light mesons in AA collisions with impact parameter $\vec{s}$ reads,

$$\int d^2q_T\,\frac{d^2\sigma_{pp\to Q}}{d^2q_T}\int d^2\tau\,T_A(s)T_A(\vec{s}-\vec{\tau})\int\limits_0^\infty dL_p\frac{dW^{AA}}{dL_p}\,\frac{\Delta E(L_p)}{E}\,\delta\left(1-z-\frac{\Delta E(L_p)}{E}\right) \quad (12)$$

The effective production length $\tilde{L}_p$ in the medium turns out to be much longer than in vacuum, because the heavy–light meson is produced mainly at the medium periphery, long distance from the hard collision point.

3.4. Data Analysis

Now we are in a position to calculate the nuclear ratio

$$R_{AA}(\vec{s},\vec{p}_T) = \frac{d^2\sigma_{AA}(s)/d^2p_T d^2s}{T_{AA}(s)\,d^2\sigma_{pp}/d^2p_T}, \quad (13)$$

to be compared with data. Here

$$T_{AA}(s) = \int d^2\tau T_A(\tau)T_A(\vec{s}-\vec{\tau}), \quad (14)$$

and $T_A(s)$ is the nuclear thickness function.

The model cannot fully predict (as well as any other model) the nuclear ratio, because the medium density is not known, but is rather the goal of the research. We embedded this information into the broadening rate (transport coefficient) following the popular model [21]

$$\hat{q}(l,\vec{s},\vec{\tau},\phi) = \frac{\hat{q}_0\, t_0}{t}\, \frac{n_{part}(\vec{s},\vec{\tau} + l\,\vec{p}_T/p_T)}{n_{part}(0,0)}\, \Theta(t - t_0)\,, \tag{15}$$

where $n_{part}(\vec{s},\vec{\tau})$ is the number of participants at transverse coordinates $\vec{s}$ and $\vec{\tau}$ relative to the centers of the colliding nuclei. The falling time dependence, $1/t$ is due to longitudinal expansion of the produced medium. The time interval t_0 required for equilibrated medium production. We fixed it at the frequently used value $t_0 = 1$ fm.

The only fitted parameter is $\hat{q}_0$, which is the maximal value of the broadening rate (transport coefficient) at $s = \tau = 0$ and $t = t_0$. In fact, measurement of this parameter is our goal. Comparison with ATLAS [16] and CMS data [22] for B-meson production (non-prompt J/ψ) in lead-lead collisions at $\sqrt{s} = 5.02$ TeV is presented in Figure 7.

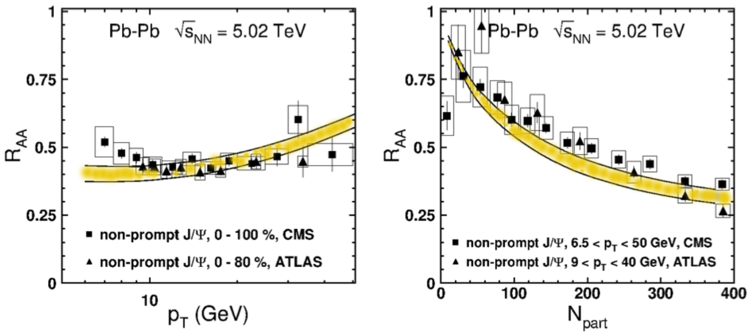

Figure 7. Nuclear ratio AA/pp for B-meson production in lead-lead collisions as function of p_T (**Left**) and versus centrality (**Right**). Data are from ATLAS [16] and CMS [22]. The strip width corresponds to the chosen interval $\hat{q}_0 = 0.2$–0.25 GeV^2/fm.

We see that data are described reasonably well, either for p_T, or N_{part} dependences, with the adjusted parameter $\hat{q}_0$ within the chosen interval $\hat{q}_0$ = 0.2–0.25 GeV^2/fm. Besides this parameter the shape of the distribution Equation (15) is very much model dependent. It is trustable only in central collisions (large n_{part}) where the medium density is close to maximal, controlled by $\hat{q}_0$. Disagreement of our predictions (if any) for peripheral collisions (small n_{part}) is out of our control, but depends mostly on the modeled form of Equation (15). For this reason, the standard fitting procedure minimizing χ^2 does not make much sense here. Instead we presented an interval for $\hat{q}_0$, providing a reasonable description of data.

Notice that the found magnitude of $\hat{q}_0$ is small compared with the values usually measured for light quarks. See discussion below.

We successfully described data on D-meson production as well, as is depicted in Figure 8.

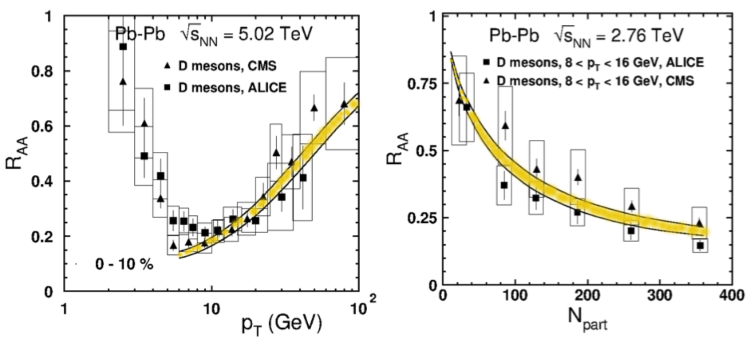

Figure 8. The same as in Figure 7, but for production of D-mesons in experiments ALICE [23] and CMS [24]. The strip width corresponds to the interval $\hat{q}_0$ = 0.45–0.55 GeV^2/fm.

Notice that c-quarks radiate in vacuum more energy than b-quarks, while the effects of absorption of $c\bar{q}$ and $b\bar{q}$ dipoles in the medium are similar. Therefore D-mesons are suppressed in AA collisions more than B-mesons. $R_{AA}(p_T)$ for D-mesons steeply rises with p_T due to color transparency. Since $b\bar{q}$ dipoles expand much faster than $c\bar{q}$, no color transparency effects are seen in $R_{AA}(p_T)$ for B-mesons, as was demonstrated in the right pane of Figure 5.

Interesting that the found broadening rate parameter for c-quarks $\hat{q}_0$ = 0.45–0.55 GeV^2/fm, significantly exceeds the value $\hat{q}_0$ = 0.2–0.25 GeV^2/fm found for b-quarks, while is quite less than $\hat{q}_0 \approx 2$ GeV^2/fm for light quarks. Such a hierarchy of broadening rates for different quark flavors would look puzzling, if $\hat{q}$ were a real transport coefficient in terms of statistical medium properties. It coincides with the rate of broadening, measured in hard reactions on nuclei only within the Born approximation [25], i.e., single gluon exchange for an inelastic process. In reality, broadening is subject to strong higher-order corrections and usually considerably exceeds the Born approximation estimate. The rate of broadening reads [26,27],

$$\hat{q} = \frac{2\pi^2}{3}\,\alpha_s(\mu^2)\,xg(x,\mu^2)\,\rho_2, \tag{16}$$

where $g(x,\mu^2)$ is the gluon density; ρ_2 is the medium density per unit of length. The characteristic scale of the process μ is related to the mean transverse momentum of the radiated gluons. For light quarks it is given by the non-perturbative effective gluon mass, $m_g \sim 0.7$ GeV [20,28]. For heavy quarks gluon radiation is subject to the dead-cone effect and the scale is much larger $\mu^2 \approx m_Q^2$. This is why the rate of broadening for heavy quarks is significantly reduced. This is another manifestation of the dead-cone effect.

The left plot in Figure 8 shows a considerable disagreement with data at small transverse momenta $p_T \lesssim 10$ GeV. While the measured $R_{AA}(p_T)$ is steeply falling with p_T, our calculations predict a nearly constant value. Such kind of disagreement has been observed earlier for light quarks, as is displayed in Figure 9.

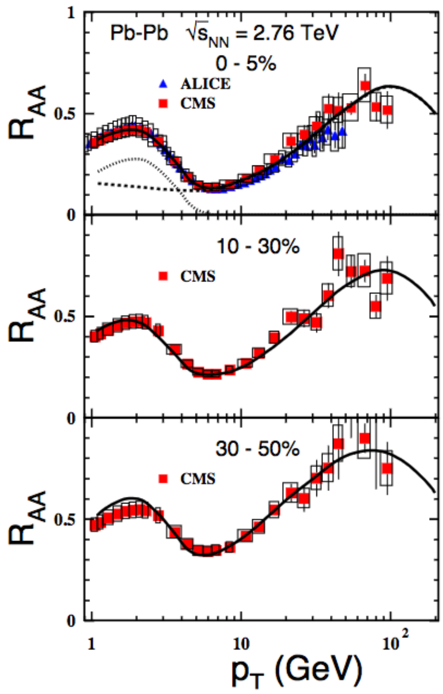

Figure 9. Suppression factor $R_{AA}(p_T)$ for lead-lead collisions at $\sqrt{s} = 2.76$ TeV vs. centrality. The dashed and dotted lines are calculated within the pQCD [29] and hydrodynamic [30] mechanisms, respectively. The solid lines represent both mechanisms summed up. Data for R_{AA} are from the ALICE [31] and CMS [32,33] experiments.

Apparently a bump at small p_T is presented in $R_{AA}(p_T)$ for D-mesons as well, while our calculations in Figure 8 disregard the hydrodynamic component.

4. Summary

Our observations and results can be summarized as follows.

- Heavy and light quarks originated from hard collisions radiate differently. The former is subject to the dead-cone effect, suppressing radiation of low-k_T gluons. Consequently heavy quarks regenerate their color field much faster than light ones and radiate a significantly smaller fraction of the initial energy. The heavier is a quark, the less it radiates.
- The fragmentation function usually depends on two variables $D_{M/q}(z, Q^2)$, fractional light-cone momentum of produced meson, and the scale Q^2. However, we consider here the case of "maximal" scale, when the jet energy and the hard scale coincide. This happens e.g., in e^+e^- annihilation, or high-p_T jet production at Feynman $x_F = 0$.
- The dead-cone effect suppressing bremsstrahlung of heavy quarks, explains the unusual shape of the fragmentation function of heavy quarks $D_{M/Q}(z)$, observed at LEP and SLAC. It peaks at large fractional momentum z, i.e., the produced heavy–light mesons, B or D, carry the main fraction of the jet momentum. On the contrary, the fragmentation function of light quarks is falling steadily with z towards $z = 1$.
- Differently from propagation of a small $q - \bar{q}$ dipole, which survives in the medium due to color transparency, a $Q - \bar{q}$ dipole promptly expands to a large transverse size, controlled by the small mass of the light quark. Such a big dipole has no chance to remain intact in a hot medium. On the other hand, a breakup of such a dipole hardly affects the production rate of $Q - \bar{q}$ mesons.
- We successfully described data on p_T and centrality dependence of the production rate of B and D mesons in heavy ion collisions. The only unavoidable parameter of such analyses is the broadening rate (usually called transport coefficient) of the quark in the medium. Its maximal value $\hat{q}_0$ was found 0.2–0.25 GeV^2/fm, 0.4–0.45 GeV^2/fm and 2 GeV^2/fm for b, c and light quarks respectively. Such hierarchy of the broadening rates is related to the same dead-cone effect. Suppression of bremsstrahlung leads to a considerable reduction of broadening.

Author Contributions: investigation, I.S.; data curation, J.N.; software, I.P.; writing—original draft preparation, B.K. All authors have read and agreed to the published version of the manuscript.

Funding: This work was supported in part by grants ANID—Chile FONDECYT 1231062 and 1230391, by ANID PIA/APOYO AFB220004, and by ANID—Millennium Science Initiative Program ICN2019_044. The work of J.N. was partially supported by Grant No. LTT18002 of the Ministry of Education, Youth and Sports of the Czech Republic, by the project of the European Regional Development Fund No. CZ.02.1.01/0.0/0.0/16_019/0000778 and by the Slovak Funding Agency, Grant No. 2/0020/22.

Conflicts of Interest: The authors declare no conflict of interest.

References

1. Casher, A.; Neubereger, H.; Nussinov, S. Chromoelectric-flux-tube model of particle production. *Phys. Rev. D* **1979**, *20*, 179–188. [CrossRef]
2. Dokshitzer, L.Y.; Khoze, V.A.; Mueller, A.H.; Troyan, S.I. *Basics of Perturbative QCD*; Tran Thanh Van, J., Ed.; Editions Frontieres: Gif-sur-Yvette, France, 1991; pp. 1–367.
3. Andersson, B. *1937 The Lund Model*; Cambridge University Press: Cambridge, UK, 1998; ISBN 0-521-42094-6 .
4. Bialas, A.; Gyulassy, M.M. Lund model and an outside-inside aspect of the inside-outside cascade. *Nucl. Phys. B* **1987**, *291*, 793–812. [CrossRef]
5. Kopeliovich, B.Z.; Niedermayer, F. Absorption of particles in nuclear matter during tunneling from vacuum. *Phys. Lett. B* **1985**, *151*, 437–438. [CrossRef]
6. Gunion, J.F.; Bertsch, G. Hadronization by color bremsstrahlung. *Phys. Rev. D* **1982**, *25*, 746–753. [CrossRef]
7. Berger, E.L. Higher Twist Effects In Deep Inelastic Scattering. *Phys. Lett. B* **1980**, 89, 241–245. [CrossRef]
8. Landau, L.D.; Pomeranchuk, I. Limits of applicability of the theory of bremsstrahlung electrons and pair production at high-energies. *Dokl. Akad. Nauk Ser. Fiz.* **1953**, *92*, 535.
9. Dokshitzer, Y.L.; Khoze, V.A.; Troian, S.I. On specific QCD properties of heavy quark fragmentation ('dead cone'). *J. Phys. G* **1991**, *17*, 1602–1604. [CrossRef]

10. Niedermayer, F. Flux tube or bremsstrahlung? *Phys. Rev. D* **1986**, *34*, 3494–3498. [CrossRef]
11. Kopeliovich, B.Z.; Potashnikova, I.K.; Schmidt, I. Why heavy and light quarks radiate energy with similar rates. *Phys. Rev. C* **2010**, *82*, 037901–037904. [CrossRef]
12. Kniehl, B.A.; Kramer, G.; Schienbein, I.; Spiesberger, H. Finite-mass effects on inclusive B meson hadroproduction. *Phys. Rev. D* **2008**, *77*, 014011–014038. [CrossRef]
13. Kneesch, T.; Kniehl, B.A.; Kramer, G.; Schienbein, I. Charmed-meson fragmentation functions with finite-mass corrections. *Nucl. Phys. B* **2008**, *799*, 34–69. [CrossRef]
14. Kopeliovich, B.Z.; Pirner, H.-J.; Potashnikova, I.K.; Schmidt, I.; Tarasov, A.V. Perturbative fragmentation. *Phys. Rev. D* **2008**, *77*, 054004–054014. [CrossRef]
15. Hwang, C.W. Charge radii of light and heavy mesons. *Eur. Phys. J. C* **2002**, *23*, 585–596. [CrossRef]
16. Aaboud, M.; Aad, G.; Abbott, B.; Abdinov, O.; Abeloos, B.; Abidi, S.H.; AbouZeid, O.S.; Abraham, N.L.; Abramowicz, H.; Abreu, H.; et al. Prompt and non-prompt J/ψ and $\psi(2S)$ suppression at high transverse momentum in 5.02 TeV Pb+Pb collisions with the ATLAS experiment. *Eur. Phys. J. C* **2018**, *78*, 762–797. [CrossRef] [PubMed]
17. Dokshitzer, Y.L.; Kharzeev, D.E. Heavy quark colorimetry of QCD matter. *Phys. Lett. B* **2001**, *519*, 199–214. [CrossRef]
18. Toki, H.; Sasaki, S.; Ichie, H.; Suganuma, H. Chiral symmetry breaking in the dual Ginzburg-Landau theory. *Austral. J. Phys.* **1997**, *50*, 199–206. [CrossRef]
19. Kopeliovich, B.Z.; Schäfer, A.; Tarasov, A.V. Bremsstrahlung of a quark propagating through a nucleus. *Phys. Rev. C* **1999**, *59*, 1609–1619. [CrossRef]
20. Kopeliovich, B.Z.; Schäfer, A.; Tarasov, A.V. Nonperturbative effects in gluon radiation and photo-production of quark pairs. *Phys. Rev. D* **2000**, *62*, 054022–054080. [CrossRef]
21. Chen, X.F.; Greiner, C.; Wang, E.; Wang, X.N.; Xu, Z. Bulk matter evolution and extraction of jet transport parameter in heavy-ion collisions at RHIC. *Phys. Rev. C* **2010**, *81*, 064908–064921. [CrossRef]
22. Sirunyan, A.M. et al. [The CMS Collaboration] Measurement of the $B^{\pm}$ Meson Nuclear Modification Factor in Pb-Pb Collisions at $\sqrt{s_{NN}} = 5.02$ TeV. *Phys. Rev. Lett.* **2017**, *119*, 152301–152305. [CrossRef]
23. Acharya, S. et al. [The CMS Collaboration] Measurement of D^0, D^+, D^{*+} and D_s^+ production in *Pb-Pb* collisions at $\sqrt{s_{NN}} = 5.02$ TeV. *J. High Energy Phys.* **2018**, *1810*, 174–209. [CrossRef]
24. Sirunyan, A.M. et al. [The CMS Collaboration] Nuclear modification factor of D^0 mesons in PbPb collisions at $\sqrt{s_{NN}} = 5.02$ TeV. *Phys. Lett. B* **2018**, *782*, 474–496. [CrossRef]
25. Baier, R.; Dokshitzer, Y.L.; Mueller, A.H.; Peigne, S.; Schiff, D. Radiative energy loss and p(T) broadening of high-energy partons in nuclei. *Nucl. Phys. B* **1997**, *484*, 265–283. [CrossRef]
26. Kopeliovich, B.Z.; Pirner, H.-J.; Potashnikova, I.K.; Schmidt, I. Mutual boosting of the saturation scales in colliding nuclei. *Phys. Lett. B* **2011**, *697*, 333–344. [CrossRef]
27. Johnson, M.B.; Kopeliovich, B.Z.; Tarasov, A.V. Broadening of transverse momentum of partons propagating through a medium. *Phys. Rev. C* **2001**, *63*, 035203–035230. [CrossRef]
28. Kopeliovich, B.Z.; Potashnikova, I.K.; Povh, B.; Schmidt, I. Evidences for two scales in hadrons. *Phys. Rev. D* **2007**, *76*, 094020–094035. [CrossRef]
29. Kopeliovich, B.Z.; Nemchik, J.; Potashnikova, I.K.; Schmidt, I. Quenching of high-pT hadrons: Energy Loss vs. Color Transparency. *Phys. Rev. C* **2012**, *86*, 054904–054921. [CrossRef]
30. Nemchik, J.; Karpenko, I.A.; Kopeliovich, B.Z.; Potashnikova, I.K.; Sinyukov, Y.M. High-pT hadrons from nuclear collisions: Unifying pQCD with hydrodynamics. In Proceedings of the 15th Conference on Elastic and Diffractive Scattering (EDS Blois 2013), Saariselka, Finland, 9–13 September 2013.
31. Abelev, B. et al. [ALICE Collaboration] Centrality dependence of charged particle production at large transverse momentum in $Pb-Pb$ collisions at $\sqrt{s} = 2.76$ TeV. *Phys. Lett. B* **2013**, *720*, 52–62. [CrossRef]
32. Lee, Y.-J. et al. [The CMS Collaboration] Quarkonia Measurements by the CMS Experiment in pp and Pb-Pb Collisions. *J. Phys. G* **2011**, *38*, 124015–124023. [CrossRef]
33. Yoon, A.S. et al. [The CMS Collaboration] Centrality and pT dependence of charged particle R_{AA} in Pb-Pb collisions at $\sqrt{s} = 2.76$ TeV. *J. Phys. G* **2011**, *38*, 124116–124122. [CrossRef]